

## HIGH TEMPERATURE FUEL AND STEAM ELECTROLYSIS CELLS USING PROTON CONDUCTIVE SOLID ELECTROLYTES

H. IWAHARA, H. UCHIDA and N. MAEDA

*Department of Environmental Chemistry and Technology, Faculty of Engineering, Tottori University, Koyamacho, Tottori 680 (Japan)*

(Received September 4, 1981; in revised form December 16, 1981)

### Summary

High-temperature-type proton conductive solids are favorable materials as electrolytes for fuel cells and steam electrolysis cells for the production of hydrogen gas.

An attempt has been made to construct a high temperature fuel cell and a steam electrolysis cell using an  $\text{SrCeO}_3$ -based solid electrolyte, which we found to be a protonic conductor in the presence of hydrogen or water vapor. Both cells could be operated stably at 800 - 1000 °C. The major limitation of the cell system was the resistance of the solid electrolytes.

---

### 1. Introduction

High temperature steam electrolysis using solid electrolytes has been considered to be an effective method of large scale hydrogen generation. When such an apparatus (an electrochemical cell) is operated inversely, it generates electric power by consuming the stored hydrogen, that is, it acts as a fuel cell. This device may be regarded as a promising direct energy converter in a future hydrogen energy system. As solid electrolytes for such a cell, oxide ion conductive ceramics, such as stabilized zirconias, have been studied by many workers [1 - 3].

High-temperature-type proton conductive solids are also favorable materials as electrolytes for such cells, and, as described below, the cells have unique advantages. However, few good high-temperature-type proton conductors are known, although several investigators have studied proton conduction in some oxides in the presence of hydrogen or water vapor at high temperatures [4 - 11]. Recently, we found that some sintered oxides based on strontium cerium trioxide exhibit appreciable proton conduction under a hydrogen containing atmosphere at high temperatures [12].  $\text{SrCe}_{0.95}\text{Y}_{0.05}\text{O}_{3-\alpha}$ ,  $\text{SrCe}_{0.95}\text{Sc}_{0.05}\text{O}_{3-\alpha}$ ,  $\text{SrCe}_{0.95}\text{Yb}_{0.05}\text{O}_{3-\alpha}$ , etc., belong to this type of conductor. ( $\alpha$  is the number of oxygen deficiencies per perovskite-type oxide unit cell.)

In this paper, some attempts to apply these materials as the electrolyte for a fuel cell and a steam electrolysis cell are described.

## 2. Operating principles — Advantages of a proton conductive solid as an electrolyte for fuel cells and steam electrolysis cells

Figure 1 illustrates the difference between the proton conductor and the oxide ion conductor in the cases of a fuel cell and steam electrolysis. In general, solid electrolytes for such cells perform the dual function of providing both ionic conduction and a diaphragm between the anode and cathode compartments. Both faces of the electrolyte have porous electrodes.

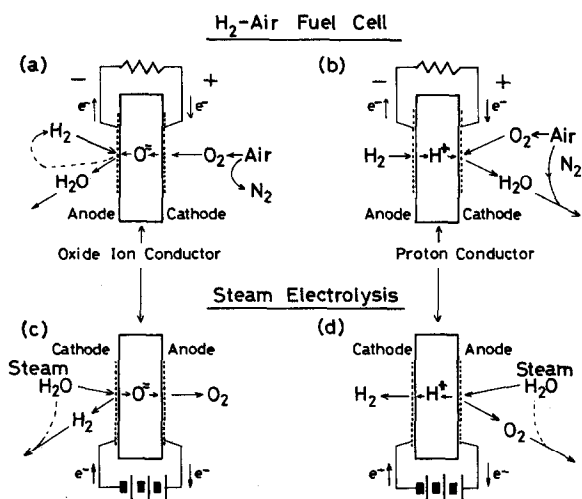
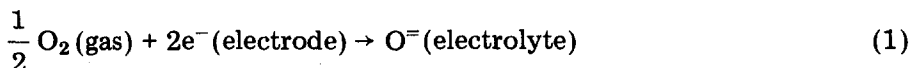


Fig. 1. Schematic illustrations of a high temperature  $H_2$  fuel cell ((a), (b)) and a steam electrolysis cell ((c), (d)). Electrolyte: oxide ion conductor, (a), (c); proton conductor, (b), (d).

### 2.1. Hydrogen-air fuel cell

In the case of an oxide ion conductor, a hydrogen-air fuel cell generates water molecules at the hydrogen electrode since oxide ions in the electrolyte migrate toward the anode, where they react with hydrogen ((a) in Fig. 1). Electrode reactions are given by

Cathode:



Anode:



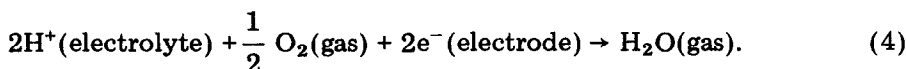
As a result, the fuel gas is diluted by water vapor, and the cell performance deteriorates unless the fuel gas is circulated to remove water vapor.

In the case of a proton conductor, on the other hand, the hydrogen-air fuel cell gives rise to water molecules at the air electrode since protons migrate from the hydrogen electrode to the air electrode, where they react with oxygen gas ((b) in Fig. 1). Electrode reactions are

Anode:



Cathode:



In this case it is unnecessary to recycle the fuel gas because water is not formed at the hydrogen electrode.

Of course, it is necessary to allow air to flow through the cathode compartment in order to avoid an accumulation of water vapor in the air electrode. However, the necessity for air flow is essential even in the case of an oxide ion conductor cell, because accumulation of nitrogen gas at the air electrode is inevitable due to the consumption of oxygen by the cell reaction.

Since the overall reaction for both cases can be written as



the e.m.f. of the cell can be written as

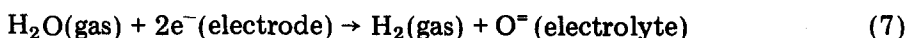
$$E = E^0 - \frac{RT}{2F} \ln \frac{P_{\text{H}_2\text{O}}}{P_{\text{H}_2} P_{\text{O}_2}^{1/2}} \quad (6)$$

where  $P_{\text{H}_2\text{O}}$ ,  $P_{\text{H}_2}$  and  $P_{\text{O}_2}$  are the partial pressures of water, hydrogen and oxygen, respectively, and  $E^0$  is determined from the change of free energy in reaction (5) at the given temperature. However, it should be noted that the meaning of  $P_{\text{H}_2\text{O}}$  is different in the two cells;  $P_{\text{H}_2\text{O}}$  refers to the cathode compartment in the case of a proton conductor, and to the anode compartment in the case of an oxide ion conductor.

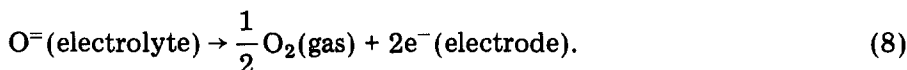
## 2.2. Steam electrolysis

In steam electrolysis using an oxide ion conductor ((c) in Fig. 1), steam is supplied to the cathode compartment of the cell, and oxygen is electrochemically extracted from  $\text{H}_2\text{O}$  in the form of oxide ions, which are forced to migrate toward the anode by the electric field applied to the electrolyte. Oxide ions discharge to produce oxygen gas at the anode. These reactions are

Cathode:



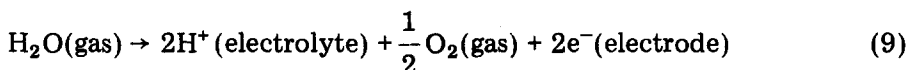
Anode:



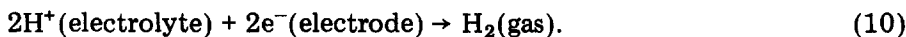
In this electrolysis, hydrogen gas obtained at the cathode is accompanied by unreacted water vapor.

Conversely, when a proton conductor is used as the electrolyte for such a cell, the steam must be introduced into the anode compartment and hydrogen is electrochemically extracted from  $\text{H}_2\text{O}$  in the form of protons, which are forced to migrate towards the cathode by the electric field ((d) in Fig. 1). Protons discharge to generate hydrogen at the cathode.

Anode:



Cathode:



Therefore, pure hydrogen without water vapor can be taken from the cathode compartment.

Consequently, the use of proton conductive solids instead of oxide ion conductors will have the following advantages: (1) pure hydrogen free from steam is available from the electrolysis; (2) fuel circulation is not necessary in the fuel cell because water molecules are not generated at the fuel electrode.

### 3. Experimental

The specimens used in this experiment consisted of  $\text{SrCe}_{1-x}\text{M}_x\text{O}_{3-\alpha}$  ( $\text{M} = \text{Sc}, \text{Yb}, x = 0.05 \text{ or } 0.10$ ). They were prepared by the solid state reaction of cerium dioxide, strontium carbonate and scandium trioxide or ytterbium trioxide. The powdered raw materials were mixed and calcined at  $1300 - 1450^\circ\text{C}$  for 10 h in air. The calcined oxides were ground and moulded by hydrostatic pressure into a column (13 mm dia.) and sintered under the above mentioned conditions. The dense sinters thus obtained were sliced into thin disks (thickness about 0.5 mm) to provide test specimens.

The construction of the solid electrolyte-gas cell (Gas I, Pt/specimen disc/Pt, Gas II) is illustrated in Fig. 2. The electrode compartments were separated by the solid electrolyte, each face of which was smeared with platinum paste and baked at  $1000^\circ\text{C}$  to provide porous electrode materials. Each electrode compartment was sealed by a glass ring packing, as shown in Fig. 2.

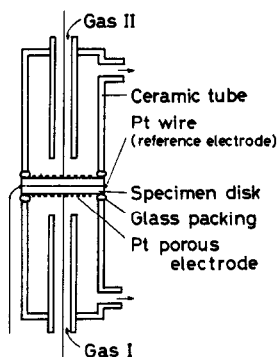


Fig. 2. Schematic diagram of test cell.

A platinum wire was attached to the side of the specimen as the reference electrode.

For the steam electrolysis cell, water vapor at 1 atm was supplied to the anode compartment, and argon gas, dried over  $P_2O_5$ , was passed through the cathode compartment to carry the evolved hydrogen gas to a detector. The hydrogen content of the exiting argon gas was from 0.3 to 8%, measured by a conventional gas chromatograph (Shimazu, Model GC-3BT, column packing: active carbon 30 - 60 mesh).

The electrode potential of the cell was measured by a conventional electrometer, a current pulse generator (Hokuto Denko, Model HC-110) was employed to correct for ohmic losses.

## 4. Results and discussion

Details of the conductivity of the specimen have been described elsewhere [12]. The protonic conductivities of these ceramics were  $10^{-3} - 10^{-2} \text{ ohm}^{-1} \text{ cm}^{-1}$  at 700 - 1000 °C, and *p*-type conduction was dominant in an atmosphere free from hydrogen or water vapor.

### 4.1. Hydrogen-air fuel cells

A hydrogen-air fuel cell was constructed using the sintered specimen as the electrolyte diaphragm and porous platinum as the electrode materials.

Typical cell performances are shown in Fig. 3. A steady and stable current could be drawn from the cell, indicating that the ceramic diaphragm could be employed as the solid electrolyte of a hydrogen-air fuel cell. Above 800 °C, the relation between terminal voltage and current output is linear. When this cell was discharged at constant current for a few hours, detectable water vapor, which condensed at the air exhaust pipe, was observed. This fact is in accordance with the protonic conduction in the specimen. As is clear from Table 1, the cell e.m.f. decreased when the cathode gas was moistened but was unaffected when the anode gas was moistened. This

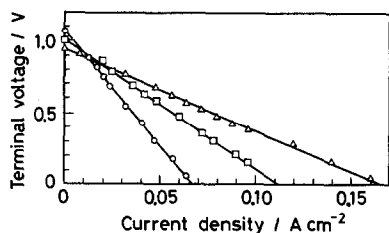


Fig. 3. Performance of the  $\text{H}_2$ ,  $\text{Pt}|\text{SrCe}_{0.95}\text{Yb}_{0.05}\text{O}_{3-\alpha}|\text{Pt}$ , Air fuel cell at 800 °C (○), 900 °C (□) and 1000 °C (△).

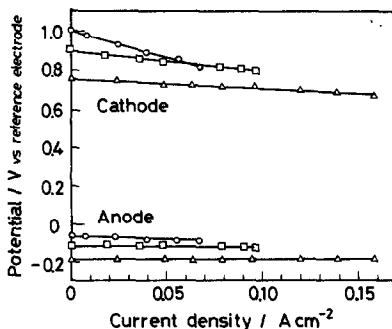


Fig. 4. Polarization of the fuel cell (excluding ohmic loss). Symbols as in Fig. 3.

TABLE 1

Effect of water vapor on the e.m.f. of the fuel cell at 800 °C  
 $\text{H}_2$ ,  $\text{Pt}|\text{Specimen electrolyte}|\text{Pt}$ , Air.

Cell type		Electrolyte	
Anode gas	Cathode gas	$\text{SrCe}_{0.95}\text{Sc}_{0.05}\text{O}_{3-\alpha}$	$\text{SrCe}_{0.95}\text{Yb}_{0.05}\text{O}_{3-\alpha}$
Wet $\text{H}_2$	Dry air	1057 (mV)	1098 (mV)
Dry $\text{H}_2$	Wet air	1047	1073
Wet $\text{H}_2$	Wet air	1047	1072

Wet gas: saturated with  $\text{H}_2\text{O}$  at room temperature (16 - 17 Torr).

Dry gas: dried over  $\text{P}_2\text{O}_5$  in the case of  $\text{SrCe}_{0.95}\text{Yb}_{0.05}\text{O}_{3-\alpha}$  and saturated with  $\text{H}_2\text{O}$  at 0 °C (4.6 Torr) in the case of  $\text{SrCe}_{0.95}\text{Sc}_{0.05}\text{O}_{3-\alpha}$ .

indicates that water molecules, the product of the cell reaction, are formed at the air electrode and that protons migrate across the solid electrolyte from the hydrogen electrode to the air electrode. This is further evidence that these ceramics have protonic conduction.

Figure 4 shows the polarization characteristics of the hydrogen and air electrodes. The potential of the hydrogen electrode corrected for ohmic loss exhibits an almost constant value against the reference electrode within the range of current output examined. At 1000 °C, little polarization was observed and cell performance depends mainly on the resistance of the electrolyte. At 800 °C, polarization of the air electrode was apparent at high current densities. Such polarization may be caused by: (1) the adsorption or accumulation of generated water molecules in the electrode reaction zone; (2) diffusion limitation of oxygen from the air to the electrode reaction zone through the pores of the electrode materials. When oxygen gas was used instead of air, a decrease in the cathodic polarization was observed. Therefore, limited oxygen diffusion may be the dominant factor in the polarization of the air electrode.

#### 4.2. Steam electrolysis cell

Steam electrolysis was carried out at 700 - 900 °C, as described in the Experimental section, using  $\text{SrCe}_{0.90}\text{Sc}_{0.10}\text{O}_{3-\alpha}$  sinters as the solid electrolyte. The evolution of hydrogen gas at the cathode on passing direct current through the cell, was confirmed by gas chromatography. The evolution of oxygen gas was also detected at the anode at half the hydrogen evolution rate. When the anode gas (1 atm water vapor) was substituted by argon dried over  $\text{P}_2\text{O}_5$ , no hydrogen was detected in the cathode gas. This supports the existence of protonic conduction in the electrolyte specimen, since the protons formed from the  $\text{H}_2\text{O}$  molecules at the anode (see eqn. (9)) must migrate across the electrolyte to discharge at the cathode (eqn. (10)).

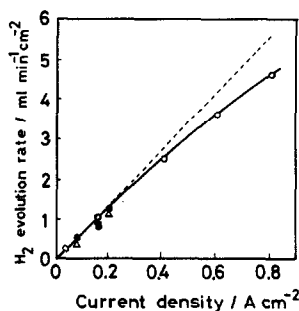


Fig. 5. Hydrogen evolution rate vs. current density at 700 °C ( $\Delta$ ), 800 °C ( $\bullet$ ) and 900 °C ( $\circ$ ). Electrolyte;  $\text{SrCe}_{0.90}\text{Sc}_{0.10}\text{O}_{3-\alpha}$  (broken line shows theoretical rate).

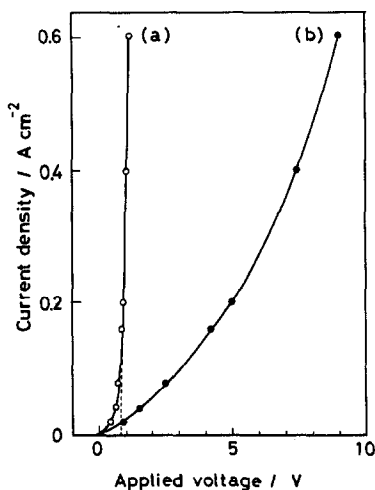


Fig. 6. Polarization curve of the steam electrolysis cell, 1 atm  $\text{H}_2\text{O}$ ,  $\text{Pt}|\text{SrCe}_{0.90}\text{Sc}_{0.10}\text{O}_{3-\alpha}|\text{Pt}$ , dry Ar at 900 °C, with (a), and without (b), correction for ohmic loss.

Figure 5 shows the dependence of the hydrogen evolution rate  $V$  ( $\text{ml min}^{-1} \text{cm}^{-2}$ ) on the electrolytic current density. The evolution rate was determined from the concentration of hydrogen,  $C$  (%), in the argon carrier gas and its flow rate  $u$  ( $\text{ml/min}$ ),

$$V = \frac{uC}{(100 - C)S} \quad (11)$$

where  $S$  is the projected electrode area ( $\text{cm}^2$ ). The theoretical evolution rate,  $V_{\text{theo}}$ , was calculated according to Faraday's law and is shown in Fig. 5 by a broken line.

The current efficiencies for  $\text{H}_2$  evolution were about 0.9 in the range 0.1 - 0.8  $\text{A/cm}^2$ . Up to 0.2  $\text{A/cm}^2$  the current efficiency seemed to be independent of the operating temperature. Current losses may be ascribed to

the electronic (hole) conduction, since the ion (proton) transport number of the specimen is not unity, as mentioned elsewhere [12].

Figure 6 shows the relation between the electrolytic current and the applied voltage with, and without, correction for ohmic loss at 900 °C. A rather high voltage was necessary to electrolyze the water vapor due to insufficient conductivity of the electrolyte specimen. However, the polarization, except for ohmic loss, was rather low, as indicated by curve (a) in Fig. 6.

The theoretical decomposition voltage for water vapor is also given by eqn. (6), in similar manner to the e.m.f. of the H<sub>2</sub>-air fuel cell. Using the thermodynamic data [13],  $E^0$  was calculated as 0.94 V at 900 °C. In order to calculate the second term of eqn. (6), the pressures of each gas ( $P_{H_2}$  and  $P_{O_2}$ ) evolving at the electrode during electrolysis must be known. We estimated the values at an electrolysis current density of 0.4 A/cm<sup>2</sup> to be  $P_{H_2} = 0.044$  atm,  $P_{O_2} = 0.022$  atm and  $P_{H_2O} = 0.978$  atm, taking the flow rate of both electrode gases to be 30 ml/min. Substituting these values into eqn. (6), we calculated the decomposition voltage of water vapor at 900 °C to be 0.7 V.

The experimental decomposition voltage obtained by extrapolating curve (a) in Fig. 4 back to zero current was 0.8 V, which was somewhat higher than that estimated from eqn. (6). However, the experimental value may be considered as being in reasonable agreement with the theoretical value if the errors caused by estimation of the partial pressures and by extrapolation of the curve are considered.

The actual applied voltage, excluding ohmic loss, was 0.95 V at 0.2 A/cm<sup>2</sup>, 1.0 V at 0.4 A/cm<sup>2</sup> and 1.2 V at 0.6 A/cm<sup>2</sup>. This indicates that the resistance due to polarization is fairly small compared with that of conventional water electrolysis. Although the conductivities of these protonic conductors are not sufficiently high (e.g.,  $5 \times 10^{-3} \Omega^{-1} \text{ cm}^{-1}$  at 900 °C for SrCe<sub>0.90</sub>Sc<sub>0.10</sub>O<sub>3- $\alpha$</sub>  [12]), they may be prospective materials if they can be used as thin films to reduce ohmic loss. For example, if the thickness of the electrolyte can be reduced to 10  $\mu\text{m}$ , the required applied voltage is 1.08 V at 0.4 A/cm<sup>2</sup> and 1.32 V at 0.6 A/cm<sup>2</sup>.

## 5. Conclusion

High temperature H<sub>2</sub>-air fuel cells and steam electrolysis cells could be constructed by using the high-temperature-type proton conductive solid electrolyte SrCe<sub>1-x</sub>M<sub>x</sub>O<sub>3- $\alpha$</sub> . The cells have, in principle, the following unique advantages: (1) fuel circulation is not necessary in the fuel cell because water molecules are not generated at the fuel electrode; (2) pure hydrogen, free from steam, is obtained from the electrolysis cell. In these cells, the polarizations, excluding ohmic loss, were relatively low compared with cells using aqueous electrolytes.

Although the conductivities of these protonic conductors are not sufficiently high, they may be prospective materials if they can be used as thin



films to reduce ohmic loss. Such a solid electrolyte cell may be used as a reciprocal direct energy converter for hydrogen  $\leftrightarrow$  electricity with high conversion efficiency in a future hydrogen energy system.

## References

- 1 H. S. Spacil and J. T. Tedman, *J. Electrochem. Soc.*, **116** (1969) 1618.
- 2 R. Accorsi and E. Bergmann, *J. Electrochem. Soc.*, **127** (1980) 804.
- 3 F. J. Rohr, in T. Takahashi and A. Kozawa (eds.), *Applications of Solid Electrolytes*, JEC Press, Cleveland, OH, 1980, p. 196.
- 4 L. Glasser, *Chem. Rev.*, **75** (1975) 21.
- 5 S. Stotz and C. Wagner, *Ber. Bunsenges. Phys. Chem.*, **70** (1966) 781.
- 6 D. A. Shores and R. A. Rapp, *J. Electrochem. Soc.*, **119** (1972) 300.
- 7 P. J. Jorgensen and F. J. Norton, *Phys. Chem. Glasses*, **10** (1969) 23.
- 8 S. White, *Nature (London)*, **225** (1970) 375.
- 9 F. Forrat, G. Dauge, P. Trévoux, G. Danner and M. Christen, *C. R. Acad. Sci.*, **259** (1964) 2813.
- 10 T. Takahashi, S. Tanase and O. Yamamoto, *Electrochim. Acta*, **23** (1978) 369.
- 11 T. Takahashi and H. Iwahara, *Rev. Chim. Miner.*, **17** (1980) 243.
- 12 H. Iwahara, T. Esaka, H. Uchida and N. Maeda, *J. Solid State Ionics*, **3/4** (1981) 359.
- 13 C. J. West, *International Critical Tables*, Vol. VII, McGraw-Hill, New York, 1930, p. 231.